Journal of Renewable Materials

Tech Science Press

Steam Exploded Peanut Shell Fiber as the Filler in the Rigid Polyurethane Foams

Zehui Ju[1], Qian He[1], Tianyi Zhan[1], Haiyang Zhang[1,*], Lin Sun[1], Lu Hong[1], Xinyi Shi[2] and Xiaoning Lu[1,*]

[1]College of Materials Science and Engineering, Nanjing Forestry University, Nanjing, 210037, China.
[2]College of Biology and the Environment, Nanjing Forestry University, Nanjing, 210037, China.
[*]Corresponding Authors: Xiaoning Lu. Email:luxiaoning-nfu@126.com; Haiyang Zhang. Email: zhynjfu@njfu.edu.cn.

Abstract: In this study, steam exploded peanut shell fibers (SE-PSFs) were utilized to fabricate with rigid polyurethane foam (RPUF) in order to improve sound absorption performance and hydrothermal weather resistance. Optimized method of SE treatment, RPUF preparation and flame retardant treatment were selected to prepare SE-PSF/RPUF composites in this experiment. Physical and mechanical properties including density, water absorption capacity, thickness swelling rate, compressive strength, thermal conductivity and average sound absorption coefficient of SE-PSF/RPUF were investigated and compared with the control (PRUF). The results showed that the density, water absorption capacity, thickness swelling rate and thermal conductivity showed an increasing trend with the increase of SE-PSFs content. The strength of the composite material showed a downward trend with the increase of the SE-PSFs content. The average sound absorption coefficient of the SE-PSFs/RPUF compared with PRUF significant increased, and the average sound absorption coefficient of the SE-PSFs/RPUF with SE-PSFs 40% was 0.47. The study getted the best ratio of flame retardants for 10% EG and 3% DMMP. The oxygen index was 35.56 vol%.

Keywords: Steam explosion; peanut shell fiber; polyurethane; composite; flame retardant properties

1 Introduction

Rigid polyurethane foam (RPUF) has been widely used in packaging, beams, indoor wall carving, outdoor wall carving, pillars, imitation wood materials and so on [1-4]. However, isocyanate and polyols used by raw materials for the production of polyurethane foam come from the petrochemical industry and consume a lot of oil resources. In addition, polyurethane foam is difficult to degrade in nature, which has caused huge pollution to the environment. Meanwhile, materials show some deficiencies, such as poor heat resistance in some cases, and it is necessary to compound with other fillers to improve these properties [5]. Foamed plastics reinforced by fiber is a new trend in this field and an important research topic of foamed plastics [6-8]. Among the fillers, peanut shell was inexpensive, biodegradable and renewable, present low environmental impact and low damage to the health of people involved in their processing. Meanwhile, peanut shell is a natural polymer, which consists of cellulose, lignin, hemicellulose, and tannins. It has more groups than two hydroxyl groups per molecule, and it can be used as polyol for the preparation of PU foam [9].

Rigid polyurethane foam belongs to organic polymer materials, and the ultimate oxygen index of rigid polyurethane foam without flame retardant treatment is only about 18%, which belongs to flammable. At present, the flame retardant used in rigid polyurethane foam includes red phosphorus,

phosphate ester, polyammonium phosphate, hydroxide and so on [10-13]. In the past few years, intumescent flame retardant has evolved as a halogen-free, environment-friendly flame retardant and is widely used in engineering plastics [14]. Expanded graphite (EG), as an effective intumescent flame retardant, has attracted much attention due to its excellent flame retardant and smoke suppression properties. Expandable graphite (EG) is made from sheet graphite treated with various intercalation agents and has a layered structure. When heated to a certain temperature, EG expands rapidly, becoming a wormlike structure with huge insulation effect [15-17]. Cheng et al. [18] used EG microencapsulated by Melamine cyanurate (MCA) to improve the safety (mechanical properties improvement and fire hazard reduction) of RPUF. The results showed that the composites containing microencapsulated expandable graphite (MCEG) decompose faster and produce more smoke than the composites containing EG. However, MCA and EG have the synergistic enhancing effect on the flame retardant property of composite.

The optimal blasting process parameters were selected by steam blasting peanut shells, and the optimal formulation of polyurethane foam was obtained through a large number of pre-experiments. Steam exploded peanut shell fibers (SE-PSFs) were utilized to fabricate with rigid polyurethane foam (RPUF) in order to improve sound absorption performance and hydrothermal weather resistance. Optimized method of SE treatment, RPUF preparation and flame retardant treatment were selected to prepare SE-PSFs/RPUF composites in this experiment. Physical and mechanical properties including density, water absorption capacity, thickness swelling rate, compressive strength, thermal conductivity and average sound absorption coefficient of SE-PSFs/RPUF were investigated and compared with the control (PRUF). Furthermore, the flame retardant of the RPUF/SE-PSFs by adding fire retardant was studied, the optimum ratio of fire retardant was determined.

2 Material and Methods

2.1 Material

Veneers of poplar (*PopulusL.*) with the dimension of 400 mm × 400 mm × 2.5 mm (length × width × height) were selected in this study without any defects. They were fabricated in Wuxi senyang wood industry co. LTD in Jiangsu province. Veneers were oven dried at 103°C for two days and reach to a stable moisture content of 5 ± 3%. The Peanut shell were collected from Ganyu country of Jiangsu province of China. The initial moisture content of the material was about 13%. Polyethylene-polypropylene glycol (Polyol 4110) hydroxyl value was 430 mg KOH/g, viscosity was 2500 ± 50 mpa·s (25°C), was provided by Nanjing hongbaoli co. LTD. N-N Dimethyl Cyclohexamine (DMCHA) was industrialize, was provided by Nanjing chemical reagent co. LTD. Dichlorofluoroethane (HFC141b) was industrialize, was provided by Jiangsu research institute of chemical industry. Silicone oil (AK8803) was industrialize, was provided by Gaolsmit, Germany. H_2O was was provided by Nanjing chemical reagent co. LTD. Polymethylene polyphenyl polyisocyanate (PAPI) viscosity was 150 ~ 250 mpa·s (25°C), was provided by Nanjing chemical reagent co. LTD. Expandable graphite (EG) was taken from Obtained from TCI Shanghai Co., Ltd. , expansion ratio was 250ml/g, initial temperature was 175°C and packing density was 0.49 g/cm^3. Dimethyl methyl methyl phosphate (DMMP) was taken from Shanghai meryl chemical technology co., LTD.

2.2 Preparation of SE-PSFs

The blasting equipment used in this test was the qbs-80 steam explosion test bench produced by zhengdao bioenergy co., LTD. The pretreatment of raw material was mainly to adjust its moisture content (MC) at frist. Water was selected as the liquid for soaking materials with comprehensive consideration of environmental protection and treatment effect. The MC of raw meterials was adjusted to about 200% after 24 h immersion. The pressure of blasting equipment was set at 2.0 MPa, 2.5 MPa, 3.0 MPa, 3.5 MPa, all in 60 s. A certain amount of water was added in the steam generator during the blasting equipment. Next, the heating device was opened and the blasting chamber was heated to make the steam pressure up to the set pressure and maintain pressure. The presoaked peanut shell was added to conduct the steam explosion after reaching the set pressure, and the material was pushed into the collected room through the open

lower croer, and the blasting process of the material was completed.

2.3 Surface Morphology Observation

The surface morphology of the samples was observed using a TM 1000 (Hitachi Co. Ltd., Japan) scanning electron microscope (SEM) with an EDS system. For SEM/EDS analysis, the oven-dried samples were mounted on the stub and gold-coated with a Model E-1010/E-1020 Ion Sputter (Hitachi Co. Ltd., Japan) prior to SEM observation. The SEM/EDS micrographs were obtained with an acceleration voltage of 15 kV.

2.4 Preparation of Bicomponent Rigid Polyurethane Foam Plastics

Polyol 4110, DMCHA, HFC141b, H_2O and AK8803 were weighed in a plastic beaker according to the formula in Tab. 1. The material was stirred by ZHX-13 at high speed, and the mixture was mixed evenly. The ZHX-13 used in this test was produced by Yancheng keen mechanical equipment co., LTD. The mixture (known as white material in industry) was put in the container for later use.

Table 1: Formulations for rigid polyurethane foam

Materials	The quality of copies
Polyol 4110	60
DMCHA	2
HFC141b	30
H_2O	1
AK8803	2
PAPI	105

2.5 Preparation of RPUF/SE-PSFs

The experiment adopted the one-step foaming preparation. Add a certain amount of drying peanut shell fiber after 3.0 MPa and 60 s blasting and washing with hot water, and stir evenly, so that the peanut fiber was dispersed in polyurethane white material as much as possible, and will not cause agglomeration. Finally, a certain proportion of black PAPI (the proportion of white material and black material was 1: 1.1) was mixxed and was stired rapidly to the mixture appears white. Meanwhile, the mixture falls into the mould of the veneers of poplar and was spreaded out evenly the weneers of poplar, and then the mould surface covered veneer of poplar was puted in press with the temperature of 50ºC for 10 min. At last, mould was putted into the oven with the temperature of 105ºC for 4h, thus light peanut shell fiber wall products were obtained.

The different quality of SE-PSFs was added to prepare composite materials whose fiber content was 0, 20 wt%, 40 wt%, 60 wt% on the basis of mastering the production of polyurethane foam plastics and the quality of polyurethane was not changed. The product was shown in Fig. 1.

Figure 1: The PSF/RPUF product

2.6 Preparation of EG-RPUF/SE-PSFs

The peanut shell fiber/polyurethane foam (SE-PSFs/RPUF) compsite material with the SE-PSFs content of 40 wt% was selected to study the flame retardant performance in consideration of the need to add expanded graphite (EG). Peanut fiber and poplar veneer were soaked for 24 h with 12.5% ammonium polyphosphate, and the composite material production process was shown in section 2.4. EG addition amount was 0, 10 wt%, 15 wt%, 20 wt% and 30 wt%. According to this gradient, the EG addition amount that meets the flame retardant requirements was selected, and then the collaborative flame retardant sample of EG and DMMP was prepared. The number of flame retardant samples and the addition amount of EG and DMMP were shown in Tab. 2.

Table 2: Flame retardant samples with different addition of EG and DMMP

Number	APP soaked peanut shell fiber	EG addition amount (wt%)	DMMP addition amount (wt%)
1	No	0	0
2	Yes	0	0
3	Yes	10	0
4	Yes	15	0
5	Yes	20	0
6	Yes	30	0
7	Yes	10	3
8	Yes	10	5

2.7 The Density Test

The density test was carried out according to Chinese Standard GB/T 6343-2009. Test instruments: Electronic balance, Vernier caliper. Test method: The samples were placed at room temperature for one month. The mass and geometrical dimensions of the samples were measured. The density of the composite material with the different content of peanut shell fiber was calculated according to the formula density. Repeat the experiment five times.

2.8 The Hydroscopicity Test

The hydroscopicity test was carried out according to Chinese Standard GB/T8810-1988. Test instruments: Electronic balance, Vernier caliper. Test method: The samples were sawed into 100 mm × 100 mm × 30 mm (length × width × height), and 3 specimens were made in each group. The samples were dried to a constant mass under 110 ± 5°C. The samples were moved to the dryer and cooled to room temperature. The quality of the dried samples was weighed. The samples were filled with water with the temperature was 25 ± 2°C, and putted out to 24 h later. Dry the surface with filter paper and weight it. The water absorption rate of the samples was calculated according to formula (1). The arithmetic mean value of the sample was the test result, and two effective numbers were taken.

$$W_S = \frac{G_2 - G_1}{S} \times 100 \tag{1}$$

The W_s is water absorption per unit area (kg/m^2). The G_1 is the weight of sample before flooding (g). The G_2 is the weight of sample after flooding(g). The S is the total surface area of the sample (cm^2).

2.9 The TS(Thickness swelling) Test

The TS(Thickness swelling) test was carried out according to Chinese Standard GB/T 17657-1999. Test instruments: Water trough, Vernier caliper. Test method: The samples were sawed into 50 mm × 50 mm × 30 mm (length × width × height), and 5 samples were made in each group. The thickness of samples was measured at center point (h_1). The samples were immersed in the tank at 20 ± 2°C, and the

samples perpendicular to the horizontal plane and keep the water than on the specimen surface. The samples should be a certain distance between the bottom of the samples and the bottom of the tank. The samples were taken out, erased the surface, and measured its thickness (h_2) at the original measuring point after soaking for 24 h. The measurement must be completed within 30 min. The TS of the samples was calculated according to formula (2). The arithmetic mean value of the sample was the test result, and two effective numbers were taken.

$$T = \frac{h_2 - h_1}{h_1} \times 100\% \quad (2)$$

The T is thickness swelling rate of water (%).

2.10 The Compression Strength Test

The compression strength test was carried out according to Chinese Standard GB/T 8813-2008. Test instruments: Universal strength testing machine, Vernier caliper. Test method: The samples were made by Section 2.4. The size of the samples was 100 mm in diameter and 30 mm in height. The compression strength of the samples was tested by the universal strength testing machine. The compression speed was 3 mm/min. A total of 5 samples were tested. The arithmetic mean value of the sample was the test result, and two effective numbers were taken.

2.11 The Thermal Conductivity Test

Thermal conductivity was measured parallel to the rise direction in prismatic samples (dimensions: 10 * 10 * 2 cm^3, smaller dimension in the rise direction) using a Fox 200 heat flow meter (Laser Comp). An average temperature was set at 24ºC and a constant temperature difference (28ºC) was kept between hot and cold plates. Measurements performed in samples of the same formulation varied less than 1% among each other, as described in ASTM D2863.

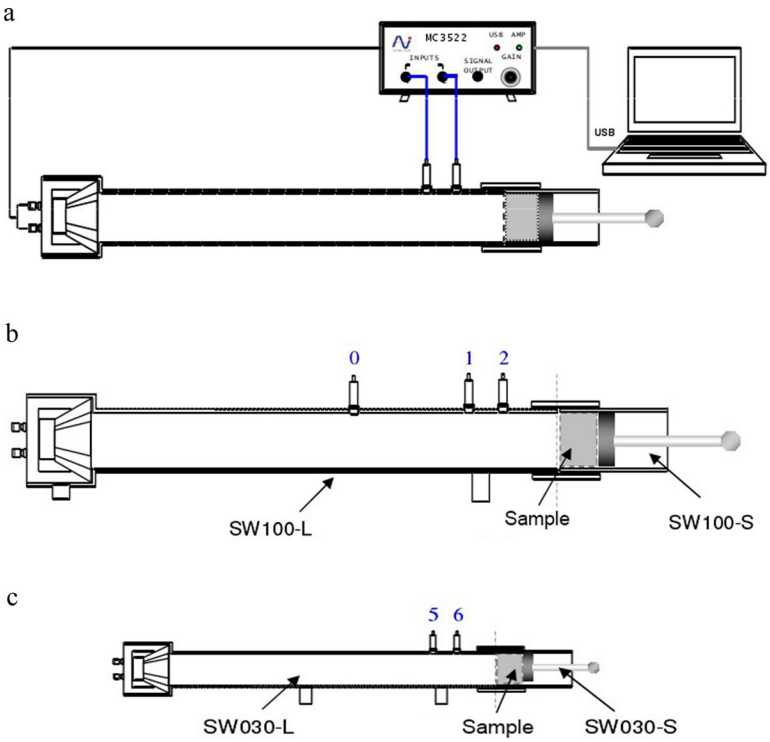

Figure 2: The sound absorption test

2.12 The Sound Absorption Test

The sound absorption test was carried out according to Chinese Standard GB/T18696.1-2004. Beijing prestige R-Cabin test system was used in the sound absorption test and the sound transmission test needs to test the transfer function of four channels as shown in Fig. 2(a). The impedance tubes are SW 422 (63 Hz to 1600 Hz) and SW 477 (800 Hz to 6300 Hz) as shown in Fig. 2(b) and Fig. 2(c). The diameter of acoustic expansion tube (SW100-L) is 100 mm, and SW100-S is 100mm. The diameter of sample is 100 mm and the thickness of sample is less than 120 mm. The diameter of acoustic expansion tube (SW030-L) is 30 mm, and SW030-S is 30 mm. The diameter of sample is 30 mm and the thickness of sample is less than 80 mm.

2.13 The Determination of Oxygen Index

The oxygen index test was carried out according to Chinese Standard GB/T8332-1987. The oxygen index of the sample was measured by JF-3 oxygen index tester. The samples were sawed into 130 mm × 10 mm × 10 mm (length × width × height), and 5 samples were made in each group. The samples of a certain size were held vertically in a transparant combustion tube where oxygen and nitrogen flow upward in proportion. Burn the top of the samples, and observe the combustion phenomenon. Record the continous combustion time or the burnt distance, and compare with the regulation value. The oxygen concentration will be reduced if the regulation was exceeded, and the oxygen concentration will be increased if the regulation was insufficient.

3 Results and Discussion

3.1 The Analysis of Blasting Results

Fig. 3 showed the fiber morphology of peanut shell under different blasting pressures. Fig. 4 showed the SEM of SE-PSFs. Some peanut shells were not blasted into fiber at the parameter of 2.0 MPa and 2.5 MPa from Fig. 3, and the peanut shell fibers were not completely separated from Fig. 4. The hydrolysis of peanut shell fibers was serious, and there were a lot of cracks and cracks on the surface of peanut shell fibers from Fig. 4. From the SEM images, it can be seen that the dissolution of granular lignin and hemicellulose adhering to the surface of fibers increases with the increase of steam explosion pressure, which is consistent with the previous research results of steam explosion treatment [19]. So, better parameters of 3.0 MPa and 60 s was selected from Fig. 3 and Fig. 4. The SE-PSFs was elongated fiber, low fiber yield, and fiber bundles were easily formed in polyurethane. Meanwhile, the probability of fibre agglomerates was relatively large. In addition, long fiber was difficult to stir in the productive process. However, the SE-PSFs to form fluffy granule was beneficial to polyurethane foam mixed foaming at 3.0 MPa.

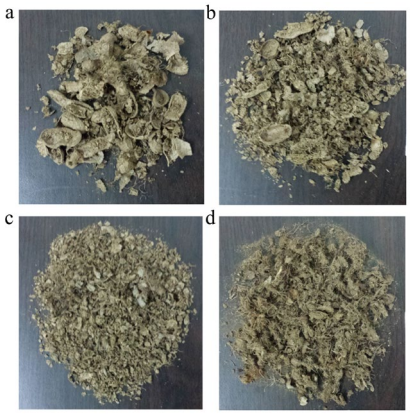

Figure 3: Peanut shell morphological characteristics after different steam explosion treatment a. 2.0 MPa, 60 s; b. 2.5 MPa, 60 s; c. 3.0 MPa, 60 s; d. 3.5 MPa, 60 s

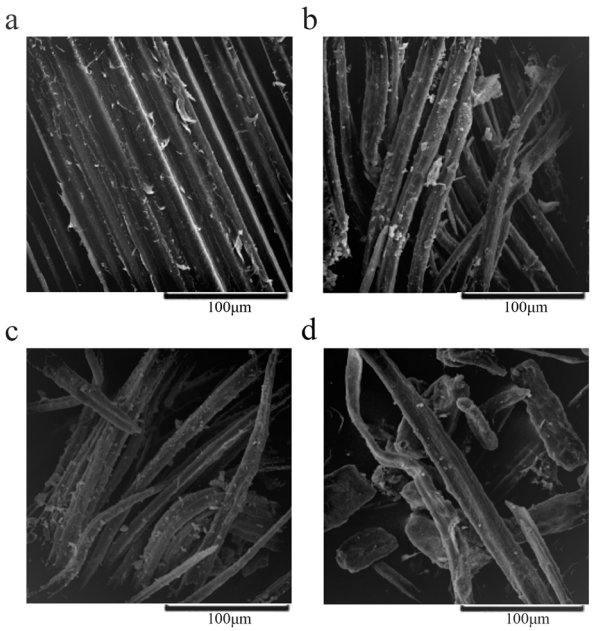

Figure 4: The SEM of SE-PSFs a. 2.0 MPa, 60 s; b. 2.5 MPa, 60 s; c. 3.0 MPa, 60 s; d. 3.5 MPa, 60 s

3.2 The Analysis of Density

RPUF foaming process had experienced several staged: the water reacted with isocyanate group generated CO_2, and gas content increased quickly in the reaction system. The newly produced gas overflow and beginned to form tiny bubbles. This process was called the bubble nucleation process, and this nucleation process became the self-nucleation process. In the actual production process, a certain amount of foam nucleating agent was added or a certain amount of gas was pre-dissolved in the reaction materials, so that the nucleation process can be carried out rapidly and continuously with a low degree of gas oversaturation. The production process made the bubble of RPUF compact and uniform. SE-PSFs had good adhesion with polyurethane matrix, and had good intermolecular force between polyurethane. Hydrogen bond was formed between the -C-O- of the fiber and the -N-H- of the polyurethane, further increasing the intermolecular.

The research showed that the density of SE-PSFs/RPUF with different peanut shell fiber contents in Tab. 3. The density of SE-PSFs/RPUF compared with RPUF increasesd obviously. When the content of SE-PSFs in steam explosion was 10%-40%, the density of SE-PSFs/RUPF doed not increase obviously. Because of the small size and large specific surface area of peanut shell fibers by steam explosion, a certain amount of small gas was adhered to the surface of peanut shell fibers. When it was added to the reaction system, it acted as an auxiliary nucleating agent and greatly increased the number of bubble nuclei in the system. In the reaction system, the number of bubbles increased, making the bubbles more compact and uniform, so that the foam grew better and increased the volume of the product under the same material [20]. The density of RPUF changed little with the increase of SE-PSFs addition. However, when the addition of SE-PSFs continues to increase, the greater the amount of SE-PSFs, the worse the compatibility. When a certain amount of PSF was added, the foaming reaction process will be affected, the original cell structure will be destroyed. The quality of the whole reaction system changes more than that of the auxiliary nucleating agent. Therefore, the density of RPUF increases gradually [21].

Table 3: The test result of samples with different peanut shell fiber contents

The fiber content of peanut shell (wt%)	0	10	20	30	40	60
Density (kg/m^3)/Standard deviation	112.33/ 0.5807	129.34/0. 8074	131.43/ 0.7582	135.02/ 0.4722	137.62/0. 5301	156.72/0. 6978
Water absorption (kg/m^2) /Standard deviation	0.81/ 0.3652	2.13/ 0.6318	2.92/ 0.7524	3.33/ 0.3128	3.52/ 0.5124	3.77/ 0.4153
Thickness swelling rate (%)/Standard deviation	1.32/ 0.7592	1.71/ 0.6234	2.03/ 0.5129	2.51/ 0.4985	2.85/ 0.5549	3.74/ 0.3964
The compressive strength of 10% relative deformation (MPa)/Standard deviation	0.282/ 0.0538	/	0.119/ 0.2954	/	0.085/ 0.1842	0.082/ 0.2943
λ(W/(m·K))/Standard deviation	0.021/ 0.0192	0.022/ 0.1568	0.023/ 0.2491	0.027/ 0.2491	0.028/ 0.0954	0.029/ 0.1252

3.3 The Analysis of Hydroscopicity

The water absorption of SE-PSFs/RPUF increased with the increase of the amount of peanut shell fiber from Tab. 3. The water absorption of SE-PSFs/RPUF compared with RPUF increasesd obviously. Due to the peanut shell fiber contains molecular groups (-OH) which was hydrophilic groups, the water absorption rate of peanut shell powder was higher than that of RPUF [22-24]. Meanwhile, with the increase of SE-PSFs content, water absorption increases smaller. It can be seen that the water absorption increased greatly when the amount of SE-PSFs increased from 0% to 10% at Tab. 3. At last, the study analyzed the variation trend of the water absorption with the density increased by considering the relation between water absorption, compression strangth, thermal insulation and sound absorption and the density.

In addition, the study also made a set of the peanut powder aontaining 60% (Screening powder by 100 mesh sieve) mixed with polyurethane foam in order to study the characteristics of SE-PSFs. The results showed that water absorption of 60% peanut powder/polyurethane foam composite was 4.27 kg/m^2, and water absorption of 60% SE-PSFs/RPUF was 3.77 kg/m^2. The results showed that the blasting peanut shell fiber had relatively good water absorption resistance ability in a certain extent. Because of most of lignin and hemicellulose was degraded to the slurry in the process of blasting, and after blasting, most of lignin, carbohydrate and other components attached to the peanut shell fiber was dissolved into the water by hot water immersion. Therefore, the peanut shell fiber prepared by blasting had better water-absorbing resistance.

3.4 The Analysis of Thickness Swelling

The thickness swelling of SE-PSFs/RPUF compared with RPUF increasesd obviously. The SE-PSFs was rich in free hydroxymethyl groups. The amorphous zone in the aggregate structure of cellulose macromolecules had strong hygroscopicity or water absorption and was easy to produce bloating [25]. It can be seen from the Tab. 3 that the TS of SE-PSFs/RPUF increased with the increase of the amount of SE-PSFs. The TS of 60% peanut powder/polyurethane foam composite was 4.79%, and TS of 60% SE-PSFs/RPUF was 3.74%. The results also indicate that the peanut shell fiber prepared by blasting had better water-absorbing resistance.

3.5 The Analysis of Compressive Strength

The compressive strength of SE-PSFs/RPUF compared with RPUF decreasesd obviously. The result

showed that the SE-PSFs/RPUF did not crush by the compressive strength test, and no maximum compressive strength. The compression strength keeped increasing and the composite material was continuously compacted. Therefore, the compressive strength of 10% relative deformation was selected to compare the compressive performance of the composite material with different amounts of peanut shell fiber. The results were shown in Tab. 3.

The compressive strength decreased from 0.282 MPa to 0.119 MPa with the peanut shell fiber content increased from 0% to 20%. Because the composite material without the peanut shell fiber foam evently, and the diameter of the bubble was small. So the compressive performance was good. The foaming of the composite material with peanut shell fiber was not uniform, bubble structure was flawed, and the diameter of the bubble was lager, so that the bubble was vulnersble to damage, and the compressive performance was degradated. As the main of the SE-PSFs/RPUF, the bubble framework beared the part of load. The smaller the bubble diameter is, the more uniform the foams are, and the better the ability of the bubble to bear the force. The compressive performance of the composite material declined when the fiber content increased. As the fiber content increased to a certain extent, it was easy to agglomerate in the PU matrix, resulting in uneven dispersion, forming a stress concentration point, local stress was too large, and the material was more likely to be damaged. Moreover, excessive fibers cannot be evenly dispersed in the resin matrix with the increase of fiber content. This leads to fiber entanglement, agglomeration and extrusion of cell, resulting in uneven cell shape and local enlargement of cell diameter. At the same time, fiber entanglement leads to reduction of resin content in some areas, poor foaming of the system and deterioration of cell structure [26].

3.6 The Analysis of Thermal Conductivity

The experimental data was shown in Tab. 3. It can be seen from the Tab. 3 that the thermal conductivity increased with the increase of fiber content. The thermal conductivity of rigid polyurethane foam was related to the density of foam plastics, the shape of foam holes, uniformity and so on. The reaction rate was relatively increased with the addition of peanut shell fiber. In this way, the bubble hole of the composite material was uniformly small, the closed hole rate was increased. The volume of composites included the volume of solids and the volume voids. At low temperature, the gas can be regarded as a static state. Only heat conduction, no convection heat transfer. Since the thermal conductivity of static air was smaller than that of solids, the thermal conductivity increased with the decrease of gaps or the increase of density (i.e., the increase of SE-PSFs content).

SE-PSFs/RPUF were compared with several common building materials in Tab. 4. It was found that the thermal conductivity of SE-PSFs/RPUF was only 1/44 of that of brick, and the thermal conductivity was very small. The SE-PSFs/RPUF also had some advantages compared to light artificial boards in these properties. These properties of SE-PSFs/RPUF were equal to polyurethane foam boards when the SE-PSFs content was 60%. Therefore, the SE-PSFs/RPUF was used as wall material, which had the excellent performance of being warm in winter and cool in summer, and can reduce energy consumption.

Table 4: The thermal conductivity of several common building materials

	Density (kg/m^3)	λ (W/(m·K))
Peanut shell fiber / polyurethane foam composite (40 wt%)	137.62	0.028
Polyurethane foam board	112.33	0.021
Light particleboard	300	0.107
Light fiberboard	260	0.124
Brick	1700	1.266
Concrete	2000	2.866

3.7 The Analysis of Sound Absorption Performance

According to the definition of sound absorption coefficient and the sound absorption mechanism of materials, the sound absorption performance of porous materials was higher than that of materials with smooth surface (most sound energy was reflected by smooth surface). The composite material with poplar veneer on the surface can be classified as board (membrane) resonance sound absorption from the sound absorption mechanism. Therefore, the sound absorption performance of SE-PSFs/RPUF with poplar veneer and composites without poplar veneer were tested in this paper.

Fig. 5(a) was the absorption coefficient of samples with poplar veneer of different SE-PSFs contents at different frequency. The peanut shell fiber content was 0%, 20%, 40% and 60%. As can be seen from the Fig. 5(a), the sound absorption coefficient of composite material covered with poplar veneer increased with the increase of the peanut shell fiber content when the sound frequency less than 500 Hz. The sound absorption coefficient of composite materials with the different content of peanut shell fiber tend to be same when the sound frequency greater than 500Hz, in addition, the sound absorption coefficient was higher than that of the low-frequency. This was mainly attributed to the sound absorption mechanism of the composite material covered with poplar veneer which can be classified as board (membrane) resonance sound absorption, and the resonance sound absorption of board (membrane) had a peak value in the low-frequency.

Fig. 5(b) showed the sound absorption coefficient of SE-PSFs/RPUF without poplar veneer at different sound frequencies. It can be seen from the Fig. 5(b) that the sound absorption coefficient of composite material without poplar veneer was much higher in high-frequency than in low-frequency. Firstly, the porous sound absorbing material had a large number of pores, small and evenly distributed porosity. The sound waves spreaded into the porous material, on the one hand, the vibration of the sound waves caused air movement between holes and holes, which made friction between acoustic wave and hole wall. Meanwhile, the porous sound absorbing material was influenced by the viscous effect, and the air vibration closing to the hole wall and solid ties was small. A considerable part of sound energy will be converted into heat energy to achieve the purpose of sound absorption under the action of friction and viscous force. On the other hand, the air and the hole wall inside the material produced heat exchange due to temperature difference, which caused heat loss and attenuated part of the sound energy. These were the two main mechanisms of sound attenuation. The vibration speed of air particles inside the material was accelerated in the high-frequency, heat exchange also was accelerated accordingly, and the friction effect was also greater. So the sound absorption performance of porous materials was very good in the high-frequency.

The average absorption coefficient of samples with different peanut shell fiber contents was shown in Tab. 5. The relation curve between the sound absorption coefficient and the peanut shell fiber contents was shown in Fig. 5(c). The relation curve between the sound absorption coefficient and the density of the composite was shown in Fig. 5(d). It can be seen from Tab. 5 that the average sound absorption coefficient of SE-PSFs/RPUF increased with the increase of SE-PSFs content. The sound absorption coefficient of the composite covered with poplar veneer was greater than 0.2 when the peanut shell fiber content was 40%, which belonged to the sound absorption material.

Table 5: The average absorption coefficient of samples with different peanut shell fiber contents

The fiber content of peanut shell (wt%)	0%	20%	40%	60%
The average absorption coefficient (coverd with poplae veneer)	0.15	0.11	0.21	0.25
The average absorption coefficient (without coverd with poplae veneer)	0.30	0.33	0.47	/

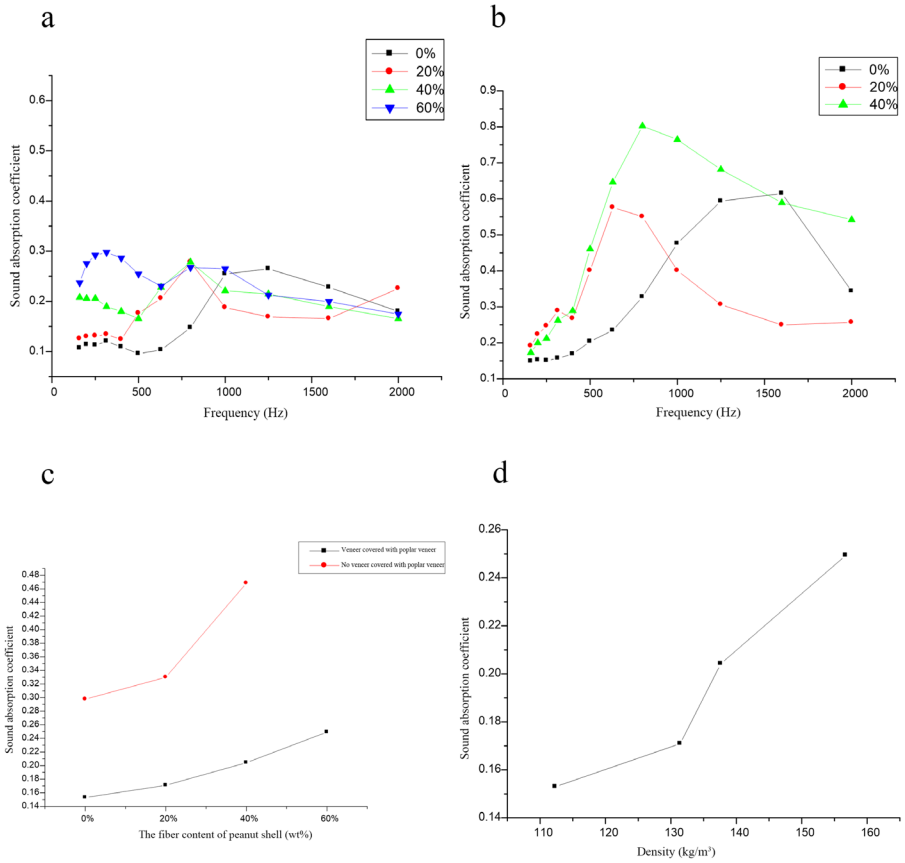

Figure 5: The sound absorption coefficient of samples

Fig. 5(c) was the average sound absorption coefficient of the SE-PSFs/RPUF covered with poplar veneer and the average sound absorption coefficient of SE-PSFs/RPUF without covered with poplar veneer. Fig. 5(c) showed that the sound absorption coefficient of composite material without poplar veneer was better than that of composite materials covered with poplar veneer. The average sound sbsorption coefficient of the SE-PSFs/RPUF with peanut shell fiber 40% was 0.47, closed to the efficient absorption material (sound absorption coefficient is greater than 0.56), so that the SE-PSFs/RPUF without poplar veneer can be used for the situation requiring high sound absorption performance. As can be seen from Fig. 5(d), the sound absorption coefficient of the composite increased with the increase of the density.

3.8 The Analysis of Oxygen Index and Observation of Combustion Process

The burned samples were photographed with a digital camera for an intuitive analysis, as shown in Fig. 6.

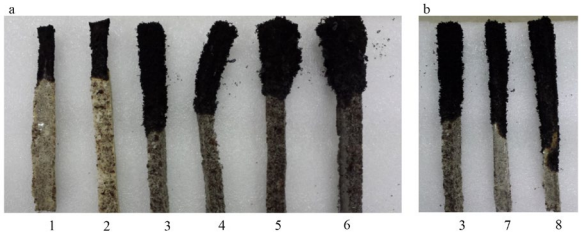

Figure 6: The combustion characteristics of samples

As shown in Fig. 6(a), the sample 1, 2 without EG was seriously shrunk after burning, indicating that the bubble hole was seriously collapsed and the internal foam was damaged. Samples 3 to 6 were the combustion characteristics with the increase of EG content, the sample without contraction has expanded volume increases gradually after combustion. In addition, the combustion surface of composite material formed a very thick carbonized layer, which can restrain further combustion of composite material to some extent. In the process of oxygen index test, carbonized layer was formed on the surface of the composite after combustion, and separated the composite from the heat source. EG was outstanding in flame-retardant performance. EG was mainly used to form a "vermicular" structure on the surface of polyurethane and form a protective layer of adiabatic and oxygen insulation to achieve the purpose of flame retardation [27]. EG was flake graphite layer structure, existed concentrated sulfuric acid between layer and layer [28]. Concentrated sulfuric acid and graphite sheet reacted to produce gas when meetting heat source. The generated gas exerted a force on the graphite sheet, maked the EG particles became "worm-like" structure covering the surface of the burning composite material, isolating air and heat sources, and achieving the purpose of flame retardant and smoke suppression. Therefore, EG can effectively improve the flame retardant performance of SE-PSFs/RPUF.

As shown in Fig. 6(b), the SE-PSFs/RPUF used EG alone produced the so-called "popcorn effect" and formed a "worm like" loose carbon layer. The burning of DMMP created phosphorus oxyacid was vitric, can be covered in the surface of combustion, formed the involatile sticky liquid membrane, increased the density and intensity of "worm" carbon layer, prevented the penetration of oxygen and heat, overcame the drawback of EG used alone, and improved flame retardant efficiency. Meanwhile, the involatile sticky liquid membrane by DMMP covered the combustion surface, maked it difficult for the toxic smoke produced by combustion to escape, and reduced the smoke release of the material.

The test results show that the oxygen index value of composite material numbered 1-8 was shown in Tab.6. The formulations of 1-8 was shown in Tab. 2.

It can be seen from Tab. 6 that the flame retardant performance increased linearly with the increase of EG content. Moreover, the composite oxygen index increased with the increase of the DMMP content and the EG 10%. It indicated that EG and DMMP had better the synergistic effect of flame retardancy. According to the test results, the oxygen index of composite material with EG additive amount of 10 wt% and DMMP additive amount of 3 wt% was up to 35.5 vol% and greater than 30 vol%, and the oxygen index of poplar veneer with 24 h soaked with ammonium polyphosphate was up to 30 vol%, both of them had reached level B1 in the international classification method of building materials' combustion performance, and met the requirements of flame retardant for building materials.

Table 6: The oxygen index of samples

Number	1	2	3	4	5	6	7	8
Oxygen index (vol%)	24.01	26.04	33.72	37.55	42.06	44.03	35.56	37.53

3.9 Effect of Flame Retardants on Properties of Composites

The density, water absorption, thickness swelling rate, the compressive strength of 10% relative deformation, thermal conductivity, and the average absorption coefficient of the SE-PSFs/RPUF with the fiber content 40% prepared with the flame retardant compound of 10wt% EG and 3wt% DMMP were tested, and the test results were compared with those of the composites without flame retardant, as shown in Tab. 7.

It can be seen from Tab. 7 that the density, water absorption and thickness swelling rate of the composite materials with flame retardant had increased. The compressive stress with a relative deformation of 10% increased from 0.085 MPa to 0.144 MPa. Thus, it can be seen that the addition of EG reduced the size of the bubble, the size of the bubble was smaller, and the mechanical properties of the composite material were good. However, the thermal conductivity of the flame-retardant composites had been improved, which indicated that the thermal insulation performance of the materials decreased, because the

thermal conductivity of EG was high. And the average sound absorption coefficient had also declined.

Table 7: Material performance comparison of add flam retardant and not add flam retardant

Test project	Composites without flame retardants	Composites with flame retardants
Density (kg/m^3)	137.62	150.61
Water absorption (kg/m^2)	3.52	3.91
Thickness swelling rate (%)	2.85	2.92
The compressive strength of 10% relative deformation (MPa)	0.085	0.144
λ (W/(m·K))	0.028	0.031

Fig. 7 showed that the sound absorption coefficient of the composite material under different frequency, the surface not covered with veneer without flame retardant of composite material sound absorption coefficient was higher than that of flame retardant. Because of EG was a very small particles, filling evently in the middle of the composite material. Therefore, there were more voids in Non-Flame-Retardant composites, that is, more air between the voids and the voids. The air movement between the voids caused friction between the acoustic wave and the void wall, so the acoustic wave was more attenuation and the absorption coefficient was larger.

4 Conclusions

In this paper, the polyurethane foamed was used as the matrix, the peanut shell fiber was used as filler by steam explosion. The properties of the composites with different contents of peanut shell fiber were studied, such as thermal insulation, sound absorption, water absorption and compression, and so on. The optimum flame retardant ratio of the SE-PSFs/RPUF was studied by adding flame retardant, and the following conclusions were obtained:

(1) The optimal blasting parameters were selected as 3.0 MPa and 60 s by steam blasting peanut shells. The best formulation of polyurethane foam was obtained by a large number of pre-experiments, and the optimal addition amount is 40%.

(2) The density, water absorption capacity and the thickness swelling rate showed an increasing trend with the increase of SE-PSFs content. The strength of the composite material showed a downward trend with the increase of the peanut shell fiber content, and the decreasing amplitude was more obvious with the peanut shell fiber content increased from 0% to 10%. The thermal conductivity also increased with the increase of peanut shell fiber. The average sound sbsorption coefficient of the PSF/RPUF with SE-PSFs 40% was 0.47, closed to the efficient absorption material (sound absorption coefficient is greater than 0.56).

(3) In this paper, research the flame retardant properties of SE-PSFs/RPUF by adding flame retardant and get the best ratio of flame retardants for 10% EG and 3% DMMP. oxygen index was 35.56 vol %.

Acknowledgement: The authors gratefully acknowledge funding supports from the National Key R&D Program of China (2017YFC0703501), the National Natural and Science Foundation (Nos. BK20170926 and BK20150878), the Postgraduate Research & Practice Innovation Program of Jiangsu Province (KYCX18_0962), the Doctorate Fellowship Foundation of Nanjing Forestry University and the Priority Academic Program Development of Jiangsu Higher Education Institutions (PAPD). LERMAB is supported by the French National Research Agency through the Laboratory of Excellence ARBRE (ANR-12- LABXARBRE-01). All authors contributed equally to this work.

References

1. Jia, F. C., Bai, Z. Q. (2015). Application of high efficiency and energy-saving polyurethane foam plastics in the exterior wall thermal insulation. *China Synthetic Resin and Plastics, 32(4),* 100-102.
2. Chattopadhyay, D. K., Raju, K. V. S. N. (2007). Structural engineering of polyurethane coatings for high performance applications. *Progress in Ploymer Science, 32(3),* 352.
3. Fu, G. Y. (2012). Construction technology of waterproofing and insulation in spraying rigid polyurethane foam on external wall. *Block-Brick-Tile, 9,* 50-51.
4. Li, P. M., Ying, W., Quan, J., Chun, Z. Z. (2015). Evaluation and selection research on external wall insulation materials based on green building energy conservation. *Materials Science Forum, 814,* 524-532.
5. Delucis, R. D. A., Petzhold, C. L., Amico, S. C. (2018). Thermal and combustion features of rigid polyurethane biofoams filled with four forest-based wastes. *Polymer Composites*.
6. Gu, R., Sain, M. M., Konar, S. K. (2013). A feasibility study of polyurethane composite foam with added hardwood pulp. *Industrial Crops and Products, 42,* 273-279.
7. Gu, R., Sain, M. M. (2013). Effects of wood fiber and microclay on the performance of soy based polyurethane foams. *Journal of Polymers and the Environment, 21,* 30-38.
8. Cao, Z. J., Dong, X., Fu, T., Deng, S. B., Liao, W. et al. (2017). Coated *vs.* naked red phosphorus: a comparative study on their fire retardancy and smoke suppression for rigid polyurethane foams. *Polymer Degradation and Stability, 136,* 103-111.
9. Bilir, M. H., Akalar, N. S., Acemioğlu, B., Baran, E., Alma, M. H. (2013). Sorption of remazol brilliant blue R onto polyurethane-type foam prepared from peanut shell. *Journal of Applied Polymer Science, 127,* 4340-4351.
10. Heinen, M., Gerbase, A. E., Petzhold, C. L. (2014). Vegetable oil-based rigid polyurethanes and phosphorylated flame-retardants derived from epoxydized soybean oil. *Polymer Degradation and Stability, 108,* 76-86.
11. Pagacz, J., Hebda, E., Michałowski, E., Ozimek, J., Sternik, D. et al. (2016). Polyurethane foams chemically reinforced with POSS-thermal degradation studies. *Thermochimica Acta, 642,* 95-104.
12. Sarier, N., Onder, E. (2007). Thermal characteristics of polyurethane foams incorporated with phase change materials. *Thermochimica Acta, 454,* 90-98.
13. Ciecierska, E., Jurczyk-Kowalska, M., Bazarnik, P., Gloc, M., Kulesza, M. et al. (2016). Flammability, mechanical properties and structure of rigid polyurethane foams with different types of carbon reinforcing materials. *Composite Structures, 140,* 67-76.
14. Li, B., Zhan, Z., Zhang, H., Sun, H. (2014). Flame retardancy and thermal performance of polypropylene treated with the intumescent flame retardant, piperazine spirocyclic phosphoramidate. *Journal of Vinyl Addittive Technology, 20,* 10-15.
15. Focke, W. W., Muiambo, H., Mhike, W., Kruger, H. J., Ofosu, O. (2014). Flexible PVC flame retarded with expandable graphite. *Polymer Degradation and Stability, 100,* 63-69.
16. Duquesne, S., Delobel, R., Le Bras, M., Camino, G. (2002). A comparative study of the mechanism of action of ammonium polyphosphate and expandable graphite in polyurethane. *Polymer Degradation and Stability, 77,* 333.
17. Modesti, M., Lorenzetti, A. (2002). Expandable graphite as an intumescent flame retardant in polyisoeyanurate-Polyurethane foams. *Polymer Degradation and Stability, 77,* 195.
18. Cheng, J. J., Qu, W. J., Sun, S. H. (2018). Mechanical properties improvement and fire hazard reduction of expandable graphite microencapsulated in rigid polyurethane foams. *Polymer Composites*.
19. Lawther, J. M., Sun, R., Banks, W. B. (1996). Effect of steam treatment on the chemical composition of wheat straw. *Holzforschung, 50,* 365-371.
20. Krishnamurthi, B., Bharadwaj, S. S., Sergeeva, T. (2003). Effect of wood flour fillers on density and mechanical properties of polyurethane foams. *Cellular Polymers, 22(6),* 371.
21. Zhang, G. Y. (2017). *Preparation and characterization of bio-based gigid polyurethane foams (Ph.D. Thesis)*. Qingdao University of Science and Technology.
22. Racz, I., Andersen, E., Aranguren, I. M., Marcovich, N. E. (2009). Wood flour-recycled polyol based polyurethane light weight composites. *Journal of Composite Materials, 43(24),* 871.
23. Song, Z. W., Liu, Y. N., Kang, W. K., Li, J. Z. (2016). Study on the preparation of polyurethane foam filled

with peanut shell. *Journal of Qingdao Agricultural University, 33(1),* 49-51.

24. Farhana, S. M. A., Mohd, H. D., Nik, N. P., Rohah, A. M. (2014). Effects of silicone surfactant on the water absorption and surface morphology of rigid palm oil-based polyurethane foam. *Applied Mechanics and Materials, 554,* 185-188.
25. Yuan, J., Shi, S. Q. (2009). Effect of the addition of wood flours on the properties of rigid polyurethane foam, *Journal of Applied Polymer Science, 113(2),* 902.
26. Luo, X., Yu, K. J., Wang, M. L., Yu, F., Qian, K. (2017). Research of glass fiber reinforced polyurethane foam performance. *New Chemistry Materials, 45,* 90-92.
27. Ge, H., Tang, H., Hu, W. Z., Wang, W. Z., Pan, Y. et al. (2015). Aluminum hypophosphite microencapsulated to improve its safety and application to flame retardant polyamide. *Journal of Hazardous Materials, 294,* 186-194.
28. Cheng, J. J., Shi, B. B., Zhou, B. B. (2014). Effects of inorganic fillers on the flame-retardant and mechanical properties of rigid polyurethane foams. *Journal of Applied Polymer Science, 131,* 376.